

# Investigation of new two-dimensional materials derived from stanene



M. Fadaie<sup>a,b</sup>, N. Shahtahmassebi<sup>a</sup>, M.R. Roknabad<sup>a</sup>, O. Gulseren<sup>b,\*</sup>

<sup>a</sup> Department of Physics, Ferdowsi University of Mashhad, Mashhad, Iran

<sup>b</sup> Department of Physics, Bilkent University, Ankara, Turkey

## ARTICLE INFO

### Article history:

Received 30 January 2017

Received in revised form 21 May 2017

Accepted 25 May 2017

### Keywords:

2D materials

Stanene

Optical properties

DFT

## ABSTRACT

In this study, we have explored new structures which are derived from stanene. In these new proposed structures, half of the Sn atoms, every other Sn atom in two-dimensional (2D) buckled hexagonal stanene structure, are replaced with a group-IV atom, namely C, Si or Ge. So, we investigate the structural, electronic and optical properties of SnC, SnGe and SnSi by means of density functional theory based first-principles calculations. Based on our structure optimization calculations, we conclude that while SnC assumes almost flat structure, the other ones have buckled geometry like stanene. In terms of the cohesive energy, SnC is the most stable structure among them. The electronic properties of these structures strongly depend on the substituted atom. We found that SnC is a large indirect band gap semiconductor, but SnSi and SnGe are direct band gap ones. Optical properties are investigated for two different polarization of light. In all structures considered in this study, the optical properties are anisotropic with respect to the polarization of light. While optical properties exhibit features at low energies for parallel polarization, there is sort of broad band at higher energies after 5 eV for perpendicular polarization of the light. This anisotropy is due to the 2D nature of the structures.

© 2017 Elsevier B.V. All rights reserved.

## 1. Introduction

In recent years, investigating the properties of the 2D structures and exploring for new stable 2D structures attract a lot of attention, so they are the focus of several studies. The first and the most remarkable material among them is graphene which is a flat honeycomb structure of carbon atoms with zero band gap and exotic topological, optical, and electronic properties [1–4]. Some of these exotic properties can be listed as half-integer and fractional quantum Hall effects [5,6], Shubnikov–de Haas oscillations with a  $\pi$  phase shift due to Berry's phase [6,7], mobility ( $\mu$ ) up to  $10^6 \text{ cm}^2 \text{ V}^{-1} \text{ s}^{-1}$  and near-ballistic transport at room temperature [8]. The novel properties and applications that emerge from 2D structure and confinement inspire the scientific community to study the other elements from the periodic table for possible graphene-like structures. For example, the 2D honeycomb structures derived from group IV elements, compounds of group III–V and II–VI are generating significant interest because of their possible unique properties that might lead several new applications. Consequently, stable 2D structures made of silicon [9–11], germanium [11] and tin [12–14] are reported, and they are named silicene, germanene and stanene, respectively. These monolayer

structures exhibit honeycomb lattice, however they are not entirely 2D but buckled structures. Recently, the 2D honeycomb structure of silicon has been realized by deposition on Ag (111) substrates [15]. Lately, experimental evidence of germanene grown by molecular beam epitaxy using a gold (111) surface as a substrate is published [16]. Moreover, boron nitride (BN), formed from the group III–V elements, in ionic honeycomb lattice is iso-structure of graphene but having insulator electronic structure, and it has also been produced [17].

Silicene and germanene have zero band gap as in the case of graphene. Even though, they have high carrier mobility, their metallic characteristics limit their application in nanoelectronics. However, stanene has a band gap in order of meV [18], so this aspect differs the stanene from the others and can make it a good candidate for several applications.

Understanding the properties of these new structures is very important, they may maintain very interesting chemical and physical properties which might lead to novel applications. In this study, we introduce new 2D hexagonal structures which are derived from stanene. First, we introduce our model and describe some numerical details. Then, structural properties are presented in details. Next, electronic properties are discussed. Last, the optical properties are studied for two direction of polarization of light. Finally, we summarize the properties of these new structures, and conclude.

\* Corresponding author.

E-mail address: [gulseren@fen.bilkent.edu.tr](mailto:gulseren@fen.bilkent.edu.tr) (O. Gulseren).

## 2. Computational details

We have performed first-principles calculations based on density-functional theory (DFT) using SIESTA package [19]. The Perdew-Burke-Ernzehof (PBE) [20] formalism of the generalized gradient approximation (GGA) is used for the exchange-correlation functional in our calculations. Because of the periodic boundary conditions, we employed a super-cell geometry in order to describe the isolated monolayer structures. A large vacuum spacing of about 20 Å is considered which ensures the interaction between the layers along z direction is negligible. We used the Monkhorst-Pack scheme for the k-point sampling. After extensive convergence test calculations, we set the k-point mesh to  $20 \times 20 \times 1$  and cutoff energy to 120 Ry. The convergence for energy is chosen as  $10^{-5}$  eV between two steps. All atomic positions were fully relaxed such that the maximum Hellmann-Feynman forces acting on each atom is less than 0.02 eV/Å upon ionic relaxation.

We have investigated the absorption properties of these new structures by calculating their frequency dependent complex dielectric function. The complex dielectric function is the linear response of a system due to external electromagnetic radiation and it is expressed the sum of real and imaginary parts as  $\varepsilon(\omega) = \varepsilon_1(\omega) + i\varepsilon_2(\omega)$ . Dielectric function calculations in SIESTA are based on the first order time dependent perturbation theory. Therefore, we first worked out the self-consistent ground-state energies and eigen functions which are used to calculate the dipolar transition matrix elements. Because of the Kramers-Kronig relation based on causality, we only need to calculate only one part, either real or imaginary, of the complex dielectric function,  $\varepsilon(\omega)$ . The imaginary part,  $\varepsilon_2(\omega)$ , is expressed by using the following equation

$$\varepsilon_2(\omega) = \frac{e^2}{\pi m^2 \omega^2} \sum_{v,c} \int_{BZ} d\vec{k} |\langle \psi_{ck} | \hat{e} \cdot \vec{p} | \psi_{vk} \rangle|^2 \delta(E_c(k) - E_v(k) - \hbar\omega) \quad (1)$$

within the dipole approximation. Here,  $c$  and  $v$  letters refer to the conduction and the valence band states, respectively.  $E_{(c,v)}(k)$  and  $\psi_{(c,v),k}$  are the corresponding energy and eigenfunction of these states. The sum runs over every pair of valance (filled) and conduction (empty) band states and the integral is over all k-points in the Brillouin zone. The electronic dipole transition matrix element is

calculated between the pair of filled and empty states where  $\hat{e}$  is the polarization vector and  $\vec{p}$  is the momentum operator. Then, the real part of the complex dielectric function can be obtained from this imaginary part,  $\varepsilon_2(\omega)$ , by using the Kramers-Kronig transformation:

$$\varepsilon_1(\omega) = 1 + \frac{2}{\pi} P \int_0^\infty \frac{\varepsilon_2(\omega') \omega'}{\omega'^2 - \omega^2} d\omega' \quad (2)$$

where  $P$  denotes the principle part [21].

The optical properties, for example the absorption spectra, can be obtained by determining the transitions from occupied to unoccupied states within the first Brillouin zone. Accordingly, the imaginary part of the dielectric function is essential and enough to describe the optical absorption which is basically calculated from the transition rate between valance and conduction band states. Therefore, once the band structure of the system is determined, i.e. eigenvalues and the eigenfunctions, the all optical constants can be calculated from the imaginary part of the complex dielectric function [18]. Eq. (1) shows the connection of the band structure to  $\varepsilon_2(\omega)$ , essentially to the optical properties. For example, the absorption coefficient  $\alpha(\omega)$  simply is

$$\alpha(\omega) = \frac{\omega}{cn(\omega)} \varepsilon_2(\omega) \quad (3)$$

where  $c$  is the speed of light and  $n$  is the refractive index which can easily be calculated from  $\varepsilon_1(\omega)$  and  $\varepsilon_2(\omega)$  as

$$n = \sqrt{\frac{\varepsilon_1^2 + \varepsilon_2^2 + \varepsilon_1}{2}}$$

Therefore,  $\varepsilon_2(\omega)$  and  $\alpha(\omega)$  are rather similar for most of the practical cases.

In the present work, the dielectric function and then the absorption coefficient are calculated in the energy interval from 0 to 20 eV for two direction of light's polarization, parallel and perpendicular to the structures. For  $\varepsilon_2(\omega)$  calculations, a denser k-point mesh, i.e.  $200 \times 200 \times 1$ , within the Monkhorst-Pack scheme is used for the Brillouin zone integrations.

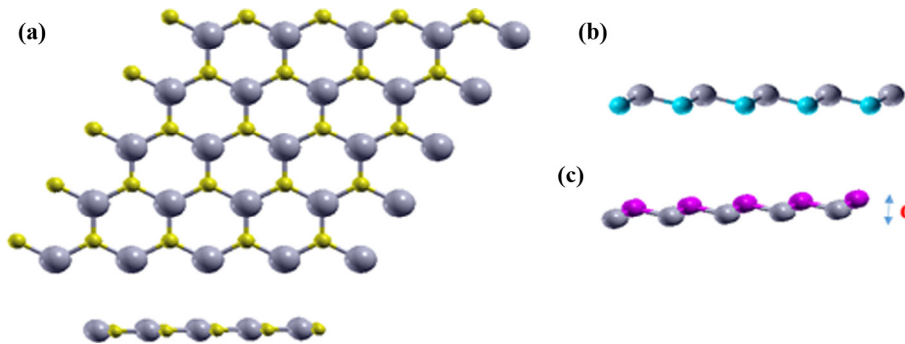


Fig. 1. (a) Top and side view of 2D SnC structure, and side view of (b) SnSi and (c) SnGe structures.

**Table 1**  
Geometrical parameters and cohesive energy of 2D SnX (X=C, Si or Ge) structures.

Structure	Bond length (Å)	Lattice parameter (Å)	Buckling length (Å)	Cohesive energy (eV)
SnC	2.11	3.66	0.01	5.52
SnSi	2.58	4.29	0.73	4.56
SnGe	2.63	4.35	0.80	4.45

### 3. Results and discussions

**Structural properties:** In order to explore the properties of these new structures, first we need to determine their geometrical structures. We defined a 2D hexagonal unit cell which consists of two atoms in the basis, one of them is Sn and the other one is C, Si or Ge. The structures are placed in xy-plane. After structural optimization, the final geometries are presented in Fig. 1. As seen in Fig. 1, SnC assumes an almost flat planar structure, while the other two, i.e. SnSi and SnGe, have quasi 2D buckled structures.

All geometrical parameters of optimized structures are summarized in Table 1. We measured the amount of non-planarity by buckling length  $d$  which is the vertical distance between two atoms in the unit cell. As seen from Table 1, the bond length between the Sn and X (C, Si or Ge) atoms, the lattice parameter and the buckling length increase with increasing atomic number of the replaced atom. All these parameters mimic the atomic radius of the constituent elements. For example, the bond length between the Sn and X is almost the sum of atomic radius of Sn and X atoms.

For this reason, it is easy to understand that SnGe structure among these structures is the most similar one to the 2D stanene structure [18].

We have calculated the cohesive energies from the total energies as

$$E_{coh} = E_T(\text{SnX}) - E_T(\text{Sn}) - E_T(\text{X})$$

where  $E_T(\text{SnX})$ ,  $E_T(\text{Sn})$  and  $E_T(\text{X})$  are respectively the total energies of 2D SnX structure, and individual Sn and X atoms placed in the same supercell as SnX. Among these three, SnC structure has the largest cohesive energy. The cohesive energies of the SnSi and SnGe, 4.56 and 4.45 eV respectively, are quite similar, while the cohesive energy of the almost planar SnC is 1 eV larger than these, 5.52 eV.

**Electronic properties:** The electronic band structure of 2D SnC, SnSi and SnGe along high symmetry directions within the Brillouin zone and their corresponding density of states (DOS) are presented in Fig. 2. The Fermi level is shifted to 0 eV in all of the diagrams. The band structure of 2D stanene exhibits linear dispersion around

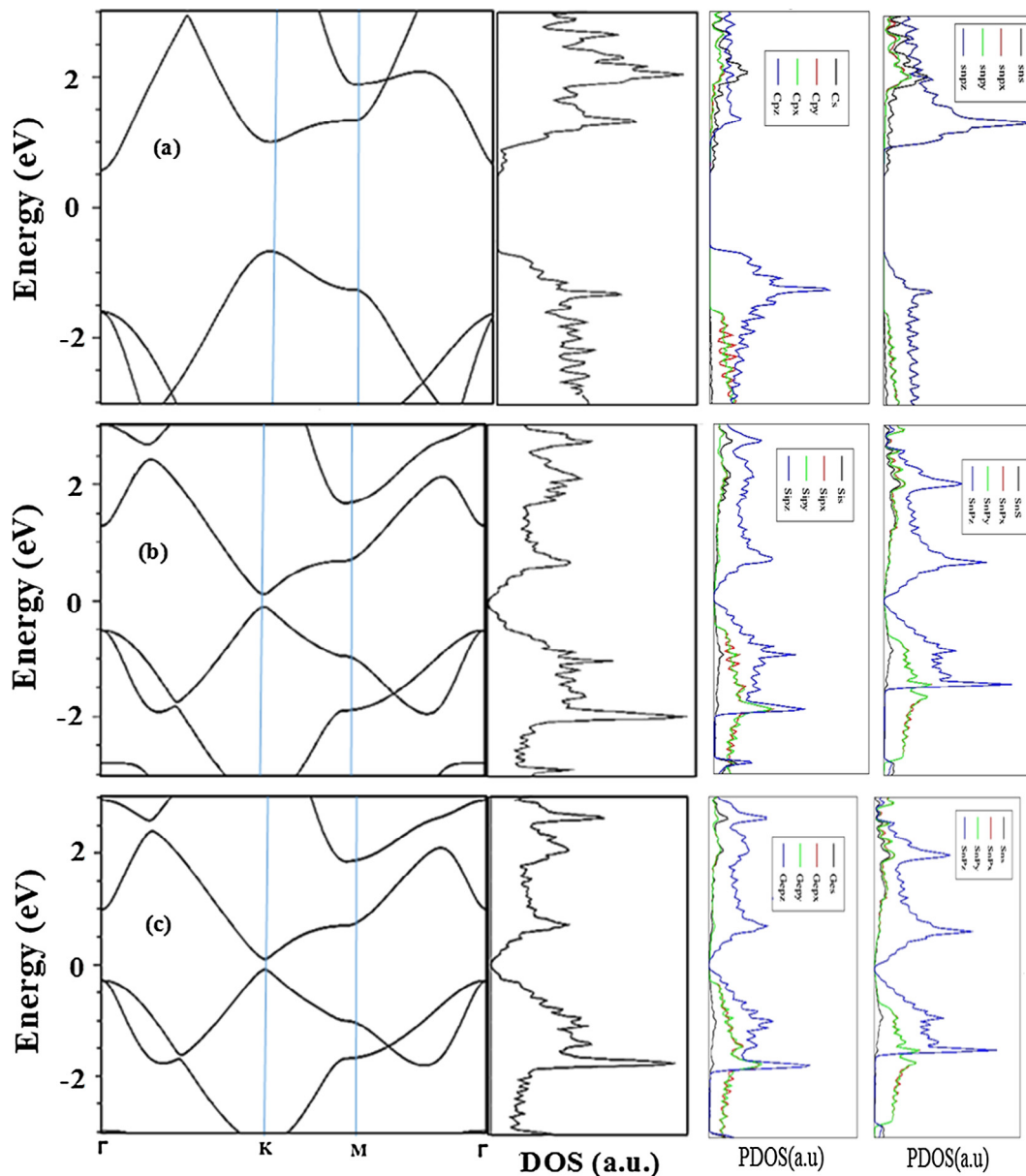


Fig. 2. Electronic band structure and density of states (total (DOS) and partial (PDOS)) of 2D (a) SnC (b) SnSi and (c) SnGe structures.

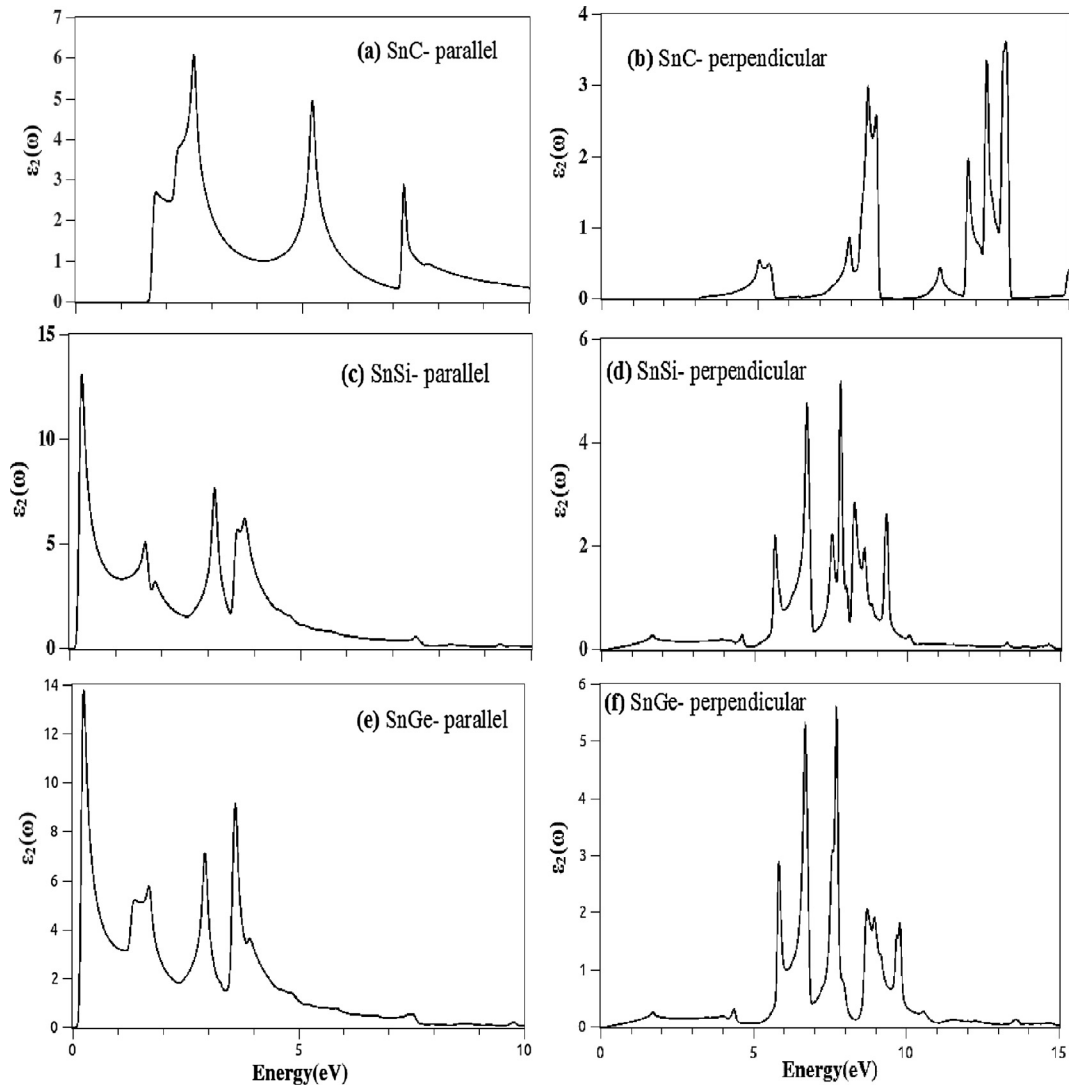


Fig. 3. The imaginary part of the complex dielectric function of 2D SnC, SnSi and SnGe structures for parallel and perpendicularly polarized light.

Fermi level with a very small bandgap of 0.04 eV at Dirac point as well as a twofold degeneracy at the valence band maximum at  $\Gamma$  point [15]. Substituting one Sn atom with C, Si or Ge atom in primitive unit cell for SnX structure changes the electronic band diagram as well as the energy bandgap. SnC is a semiconductor with a large indirect band gap of 1.5 eV between the valence band maximum at K point and the conduction band minimum at  $\Gamma$  point. On the other hand, SnSi and SnGe both have a small direct band gap, 0.21 eV and 0.23 eV respectively, between the valence and conduction band edges are both located at K point. In all structures, there is a twofold degeneracy observed at  $\Gamma$  point in valence band edge. Examination of total and projected density of states shows that while the valence band edge states exhibit C Pz character, the conduction band edge states is formed from Sn Pz orbitals in SnC structure. However, in SnSi and SnGe structures, both Sn and Si/Ge Pz orbitals character is observed at the top of valence and bottom of conduction band states. Then, the contribution from the px and py orbitals of both elements appears 0.5 eV below the valence band edge.

**Optical properties:** It is necessary to understand the optical properties of these new structures for possible optoelectronic applications. We investigated the optical properties of SnX (X=C, Si or Ge) structures in details by employing first order time-

dependent perturbation theory as described in methods section. The frequency-dependent complex dielectric function describes how light interacts with medium when it propagates through matter. The real part describes dispersion effects and the imaginary part depicts absorption.

We have calculated the optical properties for two different light polarizations, parallel to SnX plane as well as perpendicular to it. We presented the imaginary part  $\epsilon_2(\omega)$  of the complex dielectric function for both light polarization direction, i.e. parallel and perpendicular, for SnC, SnSi and SnGe structures in Fig. 3. First of all, as seen from Fig. 3,  $\epsilon_2(\omega)$  is anisotropic with respect to the polarization of light for all three structures. While  $\epsilon_2(\omega)$  exhibits features at low energies for parallel polarization, there is sort of broad band at higher energies after 5 eV for perpendicular polarization of the light. This anisotropy is due to the 2D nature of the structures. Note that, these differences with respect to the type of the light polarization are because of the selection rules dictated by the electronic dipole transition matrix elements.

For parallel polarization, basically light polarized within the 2D geometric structure, there are four (4) major peaks for all SnX structures considered here. First two peaks are due to the transitions from  $\pi$  to  $\pi^*$  states, while the following two peaks are mostly contributed by the transitions from  $\sigma$  to  $\sigma^*$  states. For example,

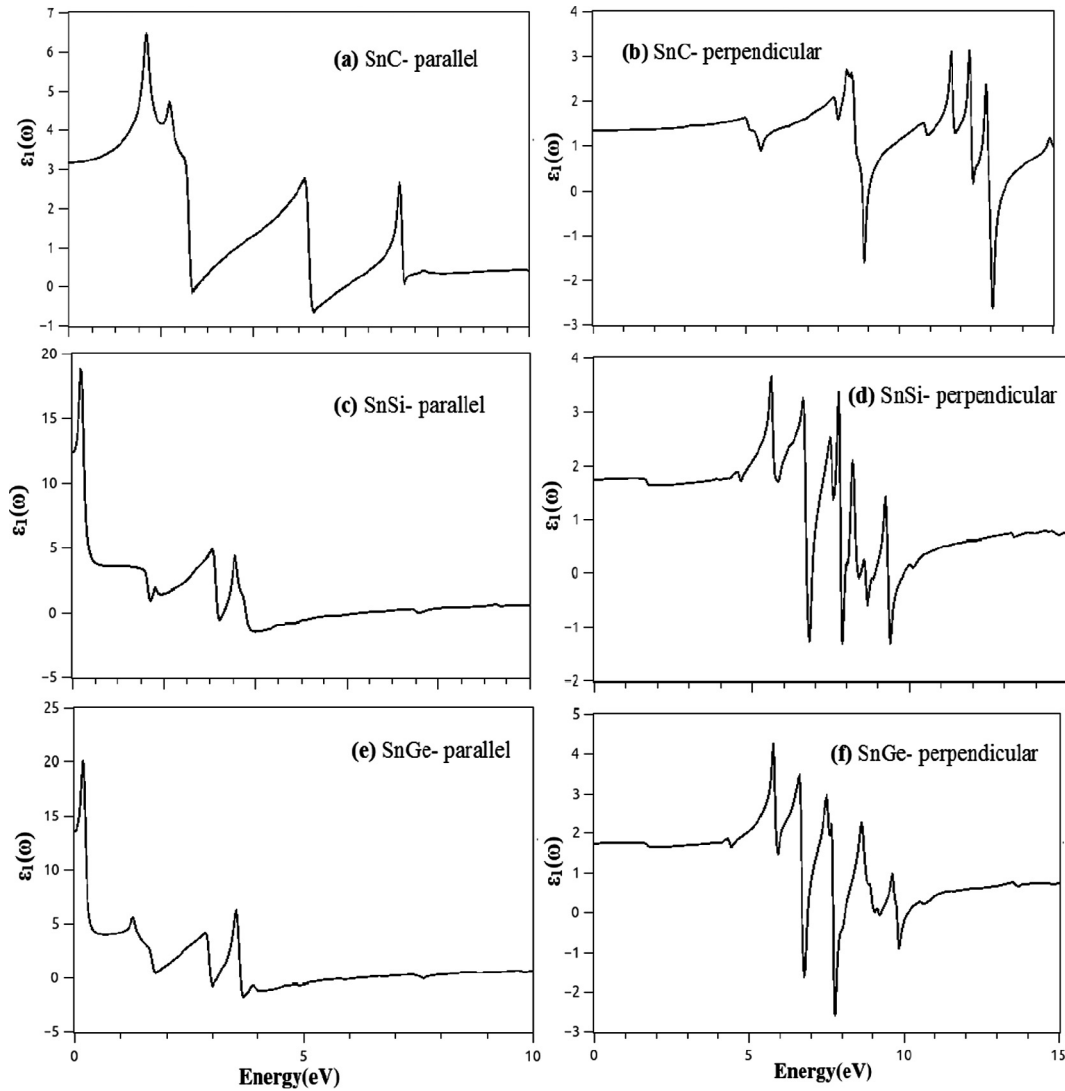


Fig. 4. The real part of the complex dielectric function of 2D SnC, SnSi and SnGe structures for parallel and perpendicularly polarized light.

the first peak is just at onset of the direct band gap, and it is arisen from  $\pi$  to  $\pi^*$  transition at K point;  $\varepsilon_2(\omega)$  is exactly zero before this. Then, the second is broad, there might be several contributions, but predominantly is arisen from  $\pi$  to  $\pi^*$  transition at M point. Then, we observe the transitions mostly from  $\sigma$  to  $\sigma^*$  states. The last, i.e. fourth, peak has quite extended tail, several eVs, indicating the contributions from many states at different k-points. After this general description, let's examine the specific structures: For  $\varepsilon_2(\omega)$  of SnC structure, the peak positions are located approximately at 1.7, 2.6, 5.1 and 7.2 eVs. The band structures of SnSi and SnGe structures are quite similar, therefore exhibits similar  $\varepsilon_2(\omega)$ , the peaks are positioned approximately at 0.2, 1.6, 3.0 and 3.8 eVs.

On the other hand, for light polarization perpendicular to the SnX structures, there are several transitions contributing to  $\varepsilon_2(\omega)$ , now we observe transitions from  $\sigma$  to  $\pi^*$  states and from  $\pi$  to  $\sigma^*$  states as well. For SnSi and SnGe structures,  $\varepsilon_2(\omega)$  is very small up to 5 eV, and then there is a broad continuous band between 5 and 10 eVs with 6 peaks. Therefore,  $\varepsilon_2(\omega)$  of these structures are quite similar to the one of stanene [18]. However, in SnC structure,  $\varepsilon_2(\omega)$  is zero till 3 eVs, and then there are 5 features including a few peaks each between 5 and 15 eVs. In this case, energy range is quite extended, i.e. 10 eVs, therefore gap regions between these features of  $\varepsilon_2(\omega)$ , i.e. it is zero.

After having the  $\varepsilon_2(\omega)$ , we used the Kramers-Kronig relation in order to calculate the real part of the complex dielectric function,  $\varepsilon_1(\omega)$  [21]. We presented the  $\varepsilon_1(\omega)$  for two different directions of light polarizations in Fig. 4. As seen in Fig. 4. in all cases, there are several peaks and dips in the real part of the complex dielectric function. Some of the dips attain small negative value, so they cross the zero. These negative values and zero crossings indicate the plasmonic excitations. For parallel polarization, these crossings are around 3 eV and 6 eV in all cases. Our calculation for perpendicularly polarized light show more number of oscillations with negative values in  $\varepsilon_1(\omega)$  compared to the case of parallel polarization of light. These negative values of the real part of dielectric function are observed at 8.5 eV and 13.5 eV for SnC structure and in the range of 5.5–10 eV for both SnSi and SnGe structures.

The optical absorption spectra of SnC, SnSi and SnGe were calculated from the complex dielectric function according to Eq. (3) for two different polarization of light, i.e. parallel and perpendicular to 2D structures. The calculated absorption coefficients,  $\alpha$ , are presented in Fig. 5. It is evident from the comparison of Figs. 3 and 5 that all features of  $\varepsilon_2(\omega)$  and  $\alpha$  are very similar. First of all, the absorption spectra of these three structures are also anisotropic with respect to the type of light polarization. Different selection rules because of the 2D geometric structure is the reason of this



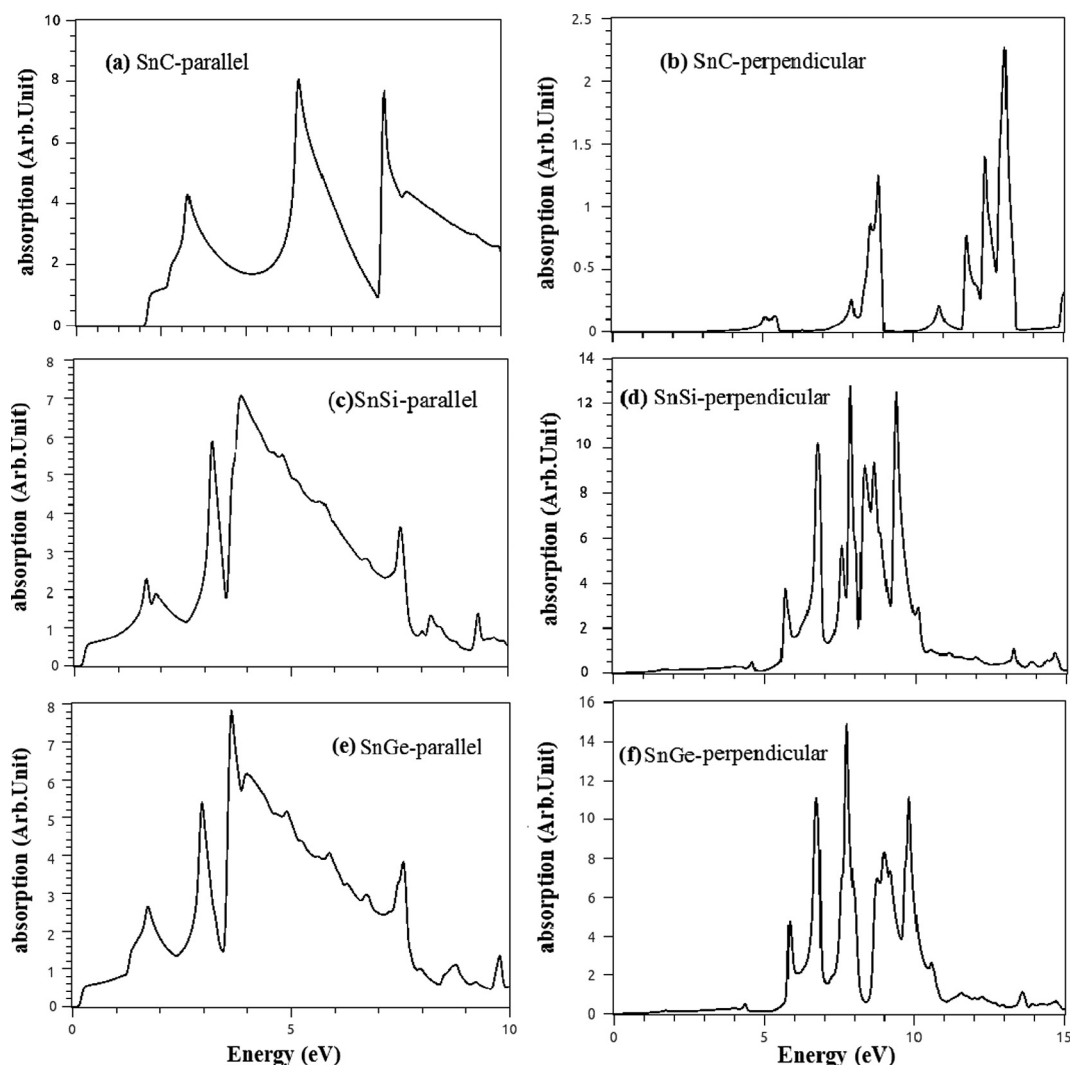


Fig. 5. Absorption spectra of 2D SnC, SnSi and SnGe structures for parallel and perpendicularly polarized light.

anisotropy. Similar to the  $\varepsilon_2(\omega)$ , absorption coefficient is zero till 1.7 eV for SnC and  $\sim 0.2$  eV for SnSi and SnGe structures, i.e. band gap region, and then exhibits a broad band extending to  $\sim 15$  eV for SnC and  $\sim 10$  eV for the other two structures. There are 3–4 peaks within this broad band corresponding the transition we described before for  $\varepsilon_2(\omega)$ . On the other hand,  $\alpha$  is almost zero till 5 eV, and then there is sort of broad band at higher energies after 5 eV for perpendicular polarization of the light. This extends till 16 eV for SnC and  $\sim 11$  eV for SnSi and SnGe structures. In general, replacing one Sn atom in the unit cell of stanene with another element of group four causes to enhancement of the peaks intensity.

#### 4. Conclusions

In summary, we have studied the structural, electronic and optical properties of new structures which are derived from stanene by substituting one of the Sn atom by another Group IV element, i.e. C, Si or Ge, based on the DFT calculations. The structural investigations show that SnC is almost planar but SnSi and SnGe has buckling, 0.73 and 0.80 Å, respectively. SnC is the most stable structure in terms of the cohesive energy. SnC is a semiconductor with a large indirect band gap of 1.5 eV between the valance band maximum at K point and the conduction band minimum at  $\Gamma$  point. On the other hand, SnSi and SnGe both have a small direct

band gap, 0.21 eV and 0.23 eV respectively, between the valance band and conduction band edges are both located at K point. All optical properties depend on the direction of light polarizations. In all structures considered in this study, the optical properties are anisotropic with respect to the polarization of light. This anisotropy is due to the 2D nature of the structures.

#### Acknowledgment

OG acknowledges the support from Scientific and Technological Research Council of Turkey (Grant no: TUBITAK-115F024).

#### References

- [1] A.K. Geim, Graphene: status and prospects, *Science* 324 (2009) 1530.
- [2] L. Liu, Z. Shen, Bandgap engineering of graphene: a density functional theory study, *Appl. Phys. Lett.* 95 (2009) 252104.
- [3] A. Lherbier, X. Blase, Y. Niquet, F. Triozon, S. Roche, Charge transport in chemically doped 2D graphene, *Phys. Rev. Lett.* 101 (2008) 036808.
- [4] D.S.L. Abergel, V. Apalkov, J. Berashevich, K. Ziegler, Tapash Chakraborty, Properties of graphene: a theoretical perspective, *Adv. Phys.* 59 (2010) 261–482.
- [5] X. Du, I. Skachko, F. Duerr, A. Luican, E.Y. Andrei, Fractional quantum Hall effect and insulating phase of Dirac electrons in graphene, *Nature* 462 (2009) 192–195.
- [6] Y. Zhang, Y. Tan, H.L. Stormer, P. Kim, Experimental observation of the quantum Hall effect and Berry's phase in graphene, *Nature* 438 (2005) 201–204.

- [7] A.K. Geim, K.S. Novoselov, The rise of graphene, *Nat. Mater.* 6 (2007) 183–191.
- [8] M.C. Lemme, T.J. Echtermeyer, M. Baus, H. Kurz, A graphene field effect device, *IEEE Electr. Device Lett.* 28 (2007) 282–284.
- [9] H. Okamoto, Y. Sugiyama, H. Nakano, Synthesis and modification of silicon nanosheets and other silicon nanomaterials, *Chem.–A Eur. J.* 17 (2011) 9864–9887.
- [10] A. Fleurence, R. Friedlein, T. Ozaki, H. Kawai, Y. Wang, Y. Yamada-Takamura, Experimental evidence for epitaxial silicene on diboride thin films, *Phys. Rev. Lett.* 108 (2012) 245501.
- [11] S. Cahangirov, M. Topsakal, E. Aktürk, H. Sahin, S. Ciraci, Two- and one-dimensional honeycomb structures of silicon and germanium, *Phys. Rev. Lett.* 102 (2009) 236804.
- [12] Y. Xu, B. Yan, H.-J. Zhang, J. Wang, G. Xu, P. Tang, W. Duan, S.-C. Zhang, Large-gap quantum spin Hall insulators in tin films, *Phys. Rev. Lett.* 111 (2013) 136804.
- [13] S. Saxena, R.P. Chaudhary, S. Shukla, Stanene: atomically thick free-standing layer of 2D hexagonal tin, *Sci. Rep.* 6 (2016) 31073.
- [14] F.F. Zhu, W.J. Chen, Y. Xu, C.-L. Gao, D.-D. Guan, C.-H. Liu, D. Qian, S.-C. Zhang, J.-F. Jia, Epitaxial growth of two-dimensional stanene, *Nat. Mater.* 14 (2015) 1020–1025.
- [15] B. Feng, Z. Ding, S. Meng, Y. Yao, X. He, P. Cheng, L. Chen, K. Wu, Evidence of silicene in honeycomb structures of silicon on Ag, *Nano Lett.* 12 (2012) 3507–3511.
- [16] M.E. Dávila, L. Xian, S. Cahangirov, A. Rubio, G. Le, Lay, Germanene: a novel two-dimensional germanium allotrope akin to graphene and silicene, *New J. Phys.* 16 (2014) 095002.
- [17] H. Şahin, S. Cahangirov, M. Topsakal, E. Bekaroglu, E. Akturk, R.T. Senger, S. Ciraci, Monolayer honeycomb structures of group-IV elements and III-V binary compounds: first-principles calculations, *Phys. Rev. B* 80 (2009) 155453.
- [18] M. Fadaie, N. Shahtahmasebi, M.R. Roknabadi, Effect of external electric field on the electronic structure and optical properties of stanene, *Opt. Quant. Electron* 48 (2016) 440.
- [19] E. Artacho, E. Anglada, O. Dieguez, J.D. Gale, A. Garcia, J. Junquera, R.M. Martin, P. Ordejon, J.M. Pruneda, D. Sanchez-Portal, J.M. Soler, The SIESTA method: developments and applicability, *J. Phys.: Condens. Matter* 20 (2008) 064208.
- [20] J.P. Perdew, K. Burke, M. Ernzerhof, Generalized gradient approximation made simple, *Phys. Rev. Lett.* 77 (1996) 3865–3868.
- [21] G. Grosso, G.P. Parravicini, *Solid State Physics*, Academic Press, 2005.